

## Cellulose acetate/nylon 66 blend membranes for pervaporation dehydration of isopropanol

Akram Kazemzadeh<sup>a</sup>, Seyed Mahmoud Mousavi<sup>b</sup>, Jamshid Mehrzad<sup>a,\*</sup>,  
Alireza Motavalizadehkakhky<sup>a</sup>, Malihesadat Hosseiny<sup>a</sup>

<sup>a</sup>Department of Chemistry, Neyshabur Branch, Islamic Azad University, 9319797139 Neyshabur, Iran, Tel./Fax: +98 51 42621944; emails: mehrzadjam@yahoo.com (J. Mehrzad), a.kazemzade@yahoo.com (A. Kazemzadeh), amotavalizadeh@yahoo.com (A. Motavalizadehkakhky), malihehosseiny@yahoo.com (M. Hosseiny)

<sup>b</sup>Chemical Engineering Department, Faculty of Engineering, Ferdowsi University of Mashhad, 9177948974 Mashhad, Iran, Tel./Fax: +98 51 38816840; email: mmousavi@um.ac.ir (S.M. Mousavi)

Received 22 August 2019; Accepted 17 March 2020

---

### ABSTRACT

Cellulose acetate (CA)/nylon 66 (NYL66) blend membranes were prepared and tested for the pervaporation separation of isopropanol (IPA) aqueous solution. These membranes were characterized through scanning electron microscopy, Fourier transform infrared spectroscopy, thermogravimetric analysis, differential scanning calorimetry, X-ray diffraction, contact angle measurement, and pervaporation test. The effects of CA/NYL66 ratio were investigated on the pervaporation performance of the membranes with the proportion of the NYL66 ranging from 0 to 20 wt.%. All blend membranes illustrated lower total flux than the pure CA membrane, while the CA/NYL66 (95/5) blend membrane had the highest separation factor and pervaporation separation index in dehydration of 80 wt.% IPA aqueous solution at 30°C.

*Keywords:* Blend membrane; Cellulose acetate; Isopropanol aqueous solution; Nylon 66; Pervaporation

---

### 1. Introduction

Pervaporation has been considered as well-established membrane technology for the dehydration of organic solvents such as alcohols [1–4], esters [5], and ketones [6] in a wide spectrum of industrial processes as well as removal of organic compounds from aqueous streams [7–9] and separation of different types of organic–organic mixtures [10–12].

Isopropanol (IPA) is one of the significant and useful types of alcohols commonly used as a solvent and cleaning agent. It has wide applications in petroleum, semiconductor, microelectronic, liquid crystal display, and pharmaceutical industries [3,13]. Furthermore, IPA is applied

as an intermediate in the production of acetone and its derivatives and also as a raw material in the manufacture of many commercial products such as glycerin [14]. An aqueous solution containing 87.9 wt.% IPA makes an azeotropic mixture [15] which in turn causes hindrance in its purification. Pervaporation is supposed to facilitate the separation of a wide variety of liquid mixtures, especially azeotropic mixtures which are difficult to be separated by conventional methods, for example, distillation and absorption [16].

A large number of hydrophilic materials have been studied for preparation of membrane for dehydration applications [17] including natural [18,19] and synthetic [20] hydrophilic polymers, and zeolites [21].

---

\* Corresponding author.

In the recent years, cellulose and its derivatives have received remarkable attention as renewable and readily available natural polymers [22]. Among these derivatives, cellulose esters resorting to its high performance and great potential for developing have attracted much research interest [23]. Cellulose acetate (CA) as an acetate ester is one of the modified natural and hydrophilic polymers which is derived from cotton linter and wood pulp [24–26]. On the other hand, CA has some disadvantages like dimensional instability and poor thermal stability [26]. A hydrophilic membrane is noticeably swelled in an aqueous solution because of water plasticizing effect which leads to the reduction of the selectivity [27]. In order to deal with these problems and intrinsic deficiencies of this polymeric membrane successfully, polymer modification could be utilized for improving its properties.

Generally, the membrane materials can be altered through three different procedures, that is, choosing various existing materials, preparing a novel material, and improving available materials [28]. More technically, blending, crosslinking, and copolymerization are commonly used methods in this regard; which among them blending method with the least required operation and a low-cost option is considered as a convenient and highly reasonable case to acquire a material with a desirable property [28].

In the same vein, CA base membranes were extensively used in various applications like ultrafiltration [29–30], pervaporation separation of organic mixtures [24–25,31] and dehydration [32–36]. The selection of a new material with respect to its compatibility with CA is a key factor for blending. In order to improve CA membrane, CA blending with other thermoplastics may be effective [26].

Nylon 66 (NYL66) is one of the most applied polymers due to its great thermal stability and high resistance to chemicals [37]. Its especial structure comprising functional group of amine and carboxylic acid that can form hydrogen bond [37], make it more efficient, and suitable for the extensive applications in such processes as microfiltration, bioassays, solvent filtration, ultrafiltration, and pervaporation [38]. More specifically, NYL66 as a mildly polar polymer can improve the thermal stability of CA and also decrease its swelling by creating a proper hydrophilic-hydrophobic balance [38,39].

In a research attempt in this respect, Sridhar et al. [39] successfully used the blend membranes of poly (vinyl alcohol) (PVA)/NYL66 for dehydration of 2-butanol–water mixtures by pervaporation. Likewise, Zhao and Huang [38] investigated the dehydration of ethanol using crosslinked blend polyacrylic acid (PAA)-NYL66 membranes and the best results were obtained from the membranes including 75 wt.% NYL66 and 25 wt.% PAA. They also found PAA is compatible with NYL66 only between ranges of 15 and 35 wt.% PAA. Furthermore, Smitha et al. [40] carried out dehydration of dioxane using chitosan/NYL66 blend membranes and demonstrated the azeotropic mixture of 1,4-dioxane/water was easily separated.

Pursuing the same line of inquiry, the present study was carried out with the aim of preparing the hydrophilic CA/NYL66 blend membranes. CA hydrophilic polymer was selected as the base polymer in pervaporation membrane for dehydration of IPA. The addition of NYL66 and CA is

to reduce the swelling, enhance of separation performance, and improve thermal stability. The obtained membranes were characterized by scanning electron microscopy (SEM), Fourier transform infrared spectroscopy (FTIR), thermogravimetric analysis and differential scanning calorimetry (TGA/DSC), X-ray diffraction (XRD), contact angle, degree of swelling (DS), and applied in pervaporation experiments.

## 2. Materials and methods

### 2.1. Materials

CA (39.8 wt.% acetyl content,  $M_n = 30,000$ ) and NYL66 were supplied by Sigma–Aldrich. Analytical grade and high purity formic acid (FA) as the solvent and IPA with an analytical purity of 97%–99% were purchased from Merck (Germany).

### 2.2. Membrane preparation

CA/NYL66 membranes were fabricated via solution casting method. In this way, blends were made in various compositions with weight ratio ranging from 95/5 to 80/20 for preparing membranes while the concentration of total polymer was adjusted to be 10%.

In preparing casting solution, the calculated amounts of two polymers were dissolved homogeneously in FA. The solution was stirred continuously for 10 h at 35°C till completely transparent mixture was obtained. After degassing, the polymer solution was cast on to a mirror plate with 350  $\mu\text{m}$  casting knife. The nascent membrane was evaporated at 40°C for 24 h. The obtained membrane was immersed in the distilled water bath and finally dried for 6 d at 40°C to remove the remaining solvent from the membrane structure before testing.

### 2.3. Scanning electron microscopy

The morphology of membranes surface was investigated using Phenom ProX SEM (Netherlands). The cross-section of the prepared membranes was characterized through LEO 1450VP SEM (Germany). Prior to this, in order to clearly cut samples, they were broken in liquid nitrogen and were coated with gold.

### 2.4. Fourier transform infrared spectroscopy studies

The existence of functional groups in membranes was identified by FTIR spectroscopy using Perkin Elmer LR 64912C FTIR spectrometer (USA) in the range of 4,000–400  $\text{cm}^{-1}$ . Spectral outputs were recorded in transmittance mode as a function of wave number.

### 2.5. Thermogravimetric analysis and differential scanning calorimetry

The simultaneous thermal analysis was conducted using Mettler Toledo TGA/DSC 1 thermogravimetric analyzer (Switzerland). The samples (about 10 mg) were heated in the temperature range of 25°C–800°C at a heating rate of 10°C/min under nitrogen atmosphere.

The degree of crystallinity can be determined from the melting peak by Eq. (1) below [13]:

$$\text{Degree of crystallinity} = \frac{\Delta H_f}{\Delta H_{f100\%}} \times 100 \quad (1)$$

where  $\Delta H_f$  is the enthalpy of melting calculated from DSC curve and  $\Delta H_{f100\%}$  is the enthalpy of melting for a fully crystalline polymer.

### 2.6. Contact angle measurements

The contact angle is used as an indicator for wettability and adopted widely as a method for investigating surface hydrophilicity. In this study, it was measured by a contact angle measuring instrument (BX51, Olympus, Japan) to evaluate surface hydrophilicity of the membranes. The reported contact angle for each sample was an average of the values for four different points of them at 25°C.

### 2.7. X-ray diffraction studies

XRD as an available technique is used primarily for characterizing crystalline polymers. It can provide useful information about crystal structure, phase, and other structural parameters. For this purpose, in the present study, an X'Pert PRO MPD X-ray diffractometer (Netherlands) was used by means of Cu-k radiation of wavelength  $\lambda = 1.54056 \text{ \AA}$  for  $2\theta$  angles between 5° and 50°.

### 2.8. Swelling experiments

The degree of membrane swelling was determined by the sorption experiments. At first, the weighed samples of circularly cut membrane pieces (3 cm diameter) were immersed in water/IPA mixture (containing 80 wt.% IPA at 30°C) during 24 h prior to measurement of swelling value. The degree of swelling (%), DS was measured by Eq. (2) [25].

$$\text{DS}(\%) = \frac{(W_s - W_d)}{W_d} \times 100 \quad (2)$$

where  $W_s$  and  $W_d$  denote the weights of a membrane in the swollen and dry state, respectively.

### 2.9. Pervaporation experiments

The setup for the pervaporation experiments is schematically shown in Fig. 1. The stainless-steel module with an effective diameter of 5 cm was utilized in the dehydration process of 1 L 80 wt.% IPA aqueous solution. The feed solution with the constant temperature of 30°C and flow rate of  $1.6 \text{ L min}^{-1}$  was pumped to the membrane surface in the permeation module. The retentate was recycled to the feed tank, and the permeate vapor, which was exposed to vacuum on the permeate side (at 10 mm Hg), was liquefied in a glass cold trap cooled with liquid nitrogen. The permeate mass through cold trap was measured by an electronic balance with 0.001 g accuracy. Furthermore, the concentration of feed and permeate was specified by measuring the refractive indexes of them using an ATAGO refractometer applying a calibration curve of concentration vs. refractive index.

The efficiency of a pervaporation membrane is usually evaluated by measuring the normalized flux ( $J$ ), separation factor ( $\alpha$ ), and pervaporation separation index (PSI), which are calculated via the following equations [41]:

$$J = \frac{m}{A \cdot t} \times l \quad (3)$$

$$\alpha = \frac{(Y_w / Y_i)}{(X_w / X_i)} \quad (4)$$

$$\text{PSI} = J(\alpha - 1) \quad (5)$$

where  $m$  is the mass of the permeate (g),  $t$  is the permeation time (h),  $A$  is the effective area of membrane ( $\text{m}^2$ ),  $l$  is membrane thickness ( $\mu\text{m}$ ),  $X$  and  $Y$  are the weight fractions of the component in the feed and permeate, and finally,  $w$  and  $i$  refer to water and IPA. In order to calculate the total flux, the mass of permeate was weighted by an electronic balance with the precision of 0.001g.

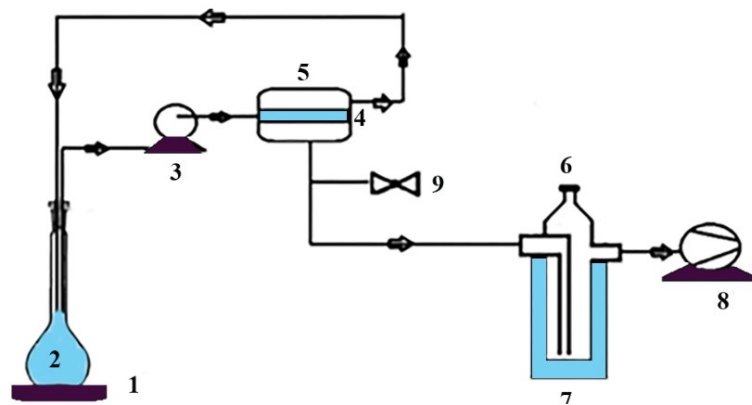


Fig. 1. Schematic diagram of pervaporation set up (1) heater, (2) feed vessel, (3) feed circulation pump, (4) membrane, (5) pervaporation module, (6) cold trap, (7) liquid nitrogen vessel, (8) vacuum pump, and (9) vacuum gauge.

### 3. Results and discussion

#### 3.1. Morphology of membranes

The morphologies of the membranes were observed using SEM. By comparing the surface SEM images of pure membranes (Fig. 2), the researcher recognized a porous surface for NYL66 membrane which was not appropriate for the pervaporation process, while the CA membrane surface was completely dense and uniform. Meanwhile, the porosity of the NYL66 membrane seem to be the result of gel formation during the evaporation of the formic acid solvent,

which leads to intense polymer interactions that in turn results in strong cross-linking [42]. Regarding the images of cross-sectional morphology of pure membranes illustrated in Fig. 2, the pure NYL66 membrane has a porous sponge-like structure, whereas the pure CA membrane is denser. Moreover, the pure membrane thickness of CA and NYL66 were about 30.5 and 53  $\mu\text{m}$ , respectively.

The surface and cross-sectional morphology of CA/NYL66 (95/5) and CA/NYL66 (90/10) blend membrane has been shown in Fig. 3. The surface of the blended membranes was dense and free-defect with no pore formation; therefore,

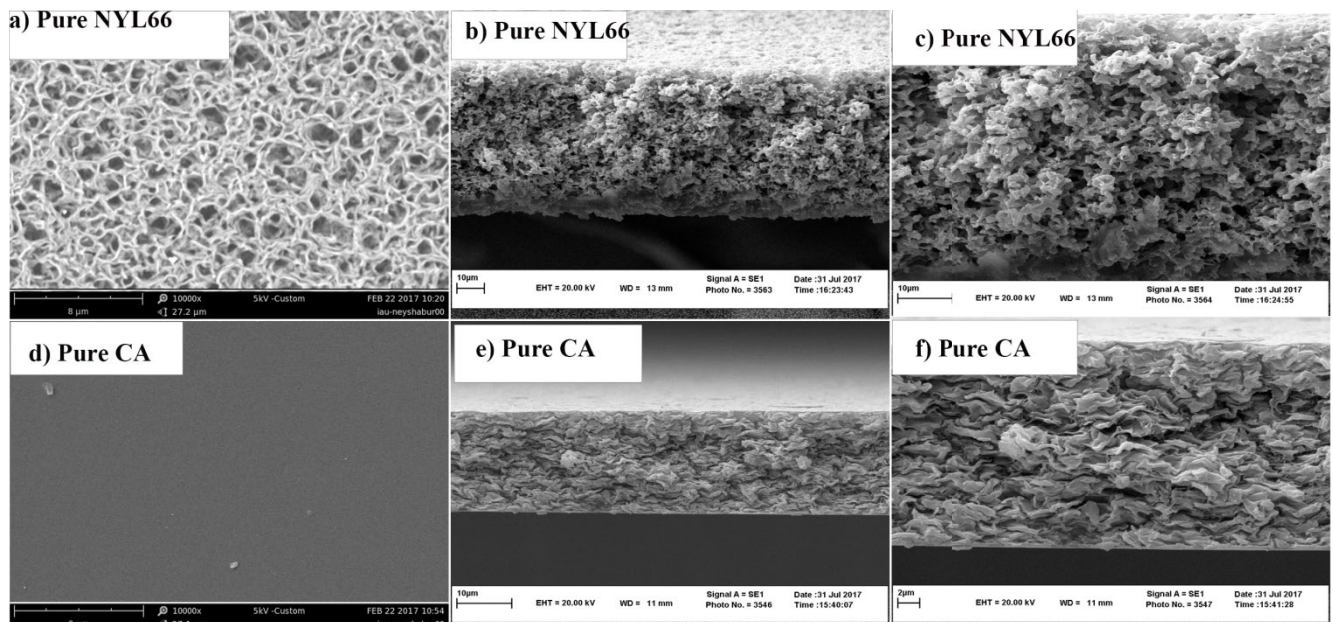


Fig. 2. SEM images of (a and d) top surface, (b and e) cross-section, and the (c and f) enlarged cross-section of pure membranes.

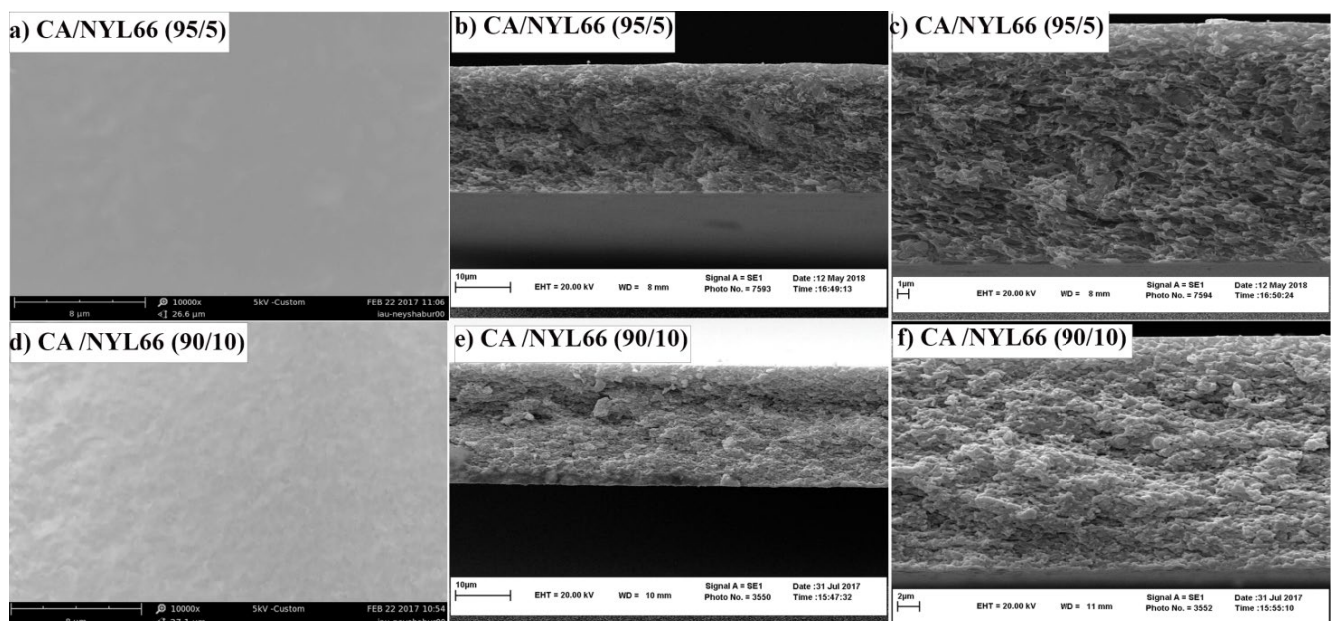


Fig. 3. SEM images of (a and d) top surface, (b and e) cross-section, and (c and f) the enlarged cross-section of the blended membranes.

they were suitable for the pervaporation process. Summing up, the thickness of the blend membranes were about 25  $\mu\text{m}$  and the surface morphology of CA/NYL66 (95/5) blend membrane was lumpy and became rougher as the content of NYL66 increased in the CA/NYL66 (90/10) blend membrane. In addition, the cross-sectional images of the blend membranes show a denser structure than the pure CA membrane. As shown in the enlarged cross-section images (Figs. 4c and f), there was no obvious difference in morphology in the top and bottom of the prepared membranes.

### 3.2. FTIR analysis

FTIR spectra of the pure and CA/NYL66 (95/5) blended membrane are indicated in Fig. 4. The spectrum of pure CA illustrates the band at 3,489  $\text{cm}^{-1}$  associated with stretching absorption of the hydroxyl group (OH) [43] and characteristic peaks of symmetric and asymmetric bending vibrations of C–H bonds in the  $\text{CH}_3$  group can be observed at 1,430 and 1,368  $\text{cm}^{-1}$  [44], respectively. Meanwhile, the existing peak in 1,763  $\text{cm}^{-1}$  represents absorption peak of carbonyl C=O [25]. Eventually, two bands placed in 905 and 604  $\text{cm}^{-1}$  can correspond to the out-of-plane bending of the hydroxyl group and vibration of  $-\text{CH}_3$  groups, respectively [44].

As observed, the pure NYL66 membrane indicates two main characteristics peak of N–H stretching [45] at 3,249  $\text{cm}^{-1}$  and carbonyl stretching band [42] at 1,737  $\text{cm}^{-1}$ . However, the present band in 1,636  $\text{cm}^{-1}$  can be also associated with combined bonds of C=O and C–N stretching vibration [39].

With respect to the FTIR spectra of the CA/NYL66 (95/5) blend membrane, it is observed that the wavenumber at

3,249  $\text{cm}^{-1}$  (N–H stretching) in the plain NYL66 has been transmitted to about 3,298  $\text{cm}^{-1}$  in the blend membrane, which can be related to the formation of an intermolecular hydrogen bonding between the hydroxyl group of CA and amide group of NYL66. The C–H band at 3,060  $\text{cm}^{-1}$  in the blend membrane is similar to that found in the pure NYL66 membrane and may be attributed to C–H stretching [46]. Additionally, two peaks associated to the C–H band are located within the range between the corresponding peaks in pure NYL66 and CA membranes (2,936–2,949  $\text{cm}^{-1}$  and 2,864–2,895  $\text{cm}^{-1}$ ). The wave number of the carbonyl group in the pure CA membrane is higher than that of NYL66. This parameter is increased in the blend membranes in comparison with the pure NYL66 membrane. This transmission of C=O to higher wavelength numbers exhibits a further increase in the number of acetyl carbonyl units in the blend membranes than the pure NYL66 membrane. Moreover, this transfer could be due to the formation of new N–H...O bonding (between C=O band of CA with N–H functional group of NYL66) and also O–H...O hydrogen bond (between C=O group in NYL66 with O–H functional group in CA). More importantly, the existence of such an intermolecular force can be a good reason for the miscibility between two polymers [25].

### 3.3. DSC studies

DSC was employed to characterize the thermal behavior of pure membranes and CA/NYL66 (95/5) blended membrane. Fig. 5 shows DSC thermograms of the membranes. As it is illustrated, the pure NYL66 membrane has an explicit melting point ( $T_m$ ) of about 264°C that is related

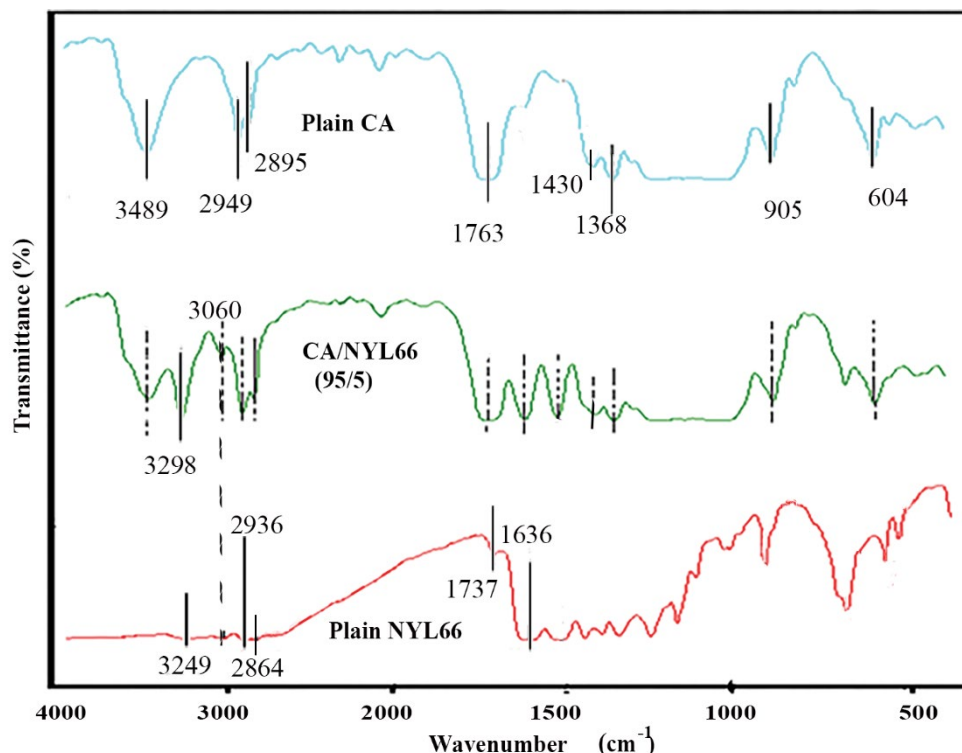


Fig. 4. FTIR spectra of the pure membranes and the CA/NYL66 (95/5) blend membrane.

to the alpha phase and is similar to the findings of other researchers [47,48]. Moreover, the glass transition temperature ( $T_g$ ) of the NYL66 membrane is about 217°C. With respect to the DSC thermograph, the melting enthalpy of the pure NYL66 membrane,  $\Delta H_f$  is 57.90 J g<sup>-1</sup>, and the melting enthalpy ( $\Delta H_{f100\%}$ ) of fully crystalline NYL66 is 197 J g<sup>-1</sup> as taken from the literature [48]. Therefore, the degree of crystallinity of the NYL66 membrane is calculated (Eq. 1) about 30%.

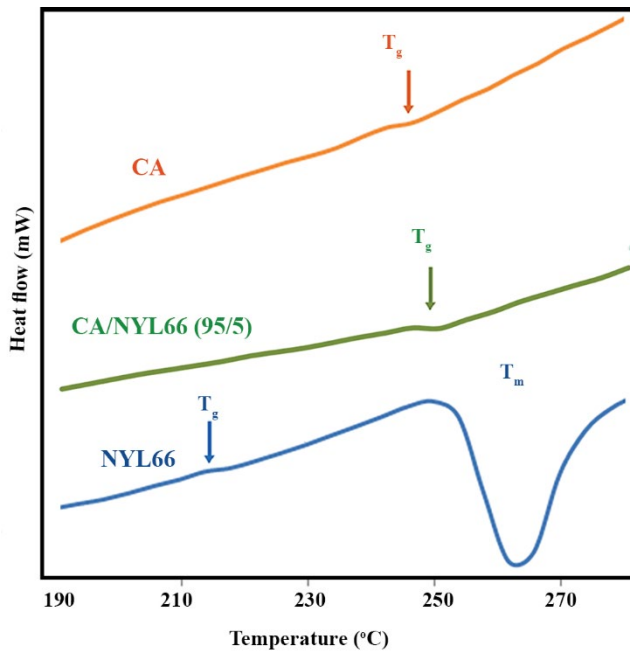


Fig. 5. DSC curves of the pure membranes and the CA/NYL66 (95/5) blend membrane.

As presented in Fig. 5, the  $T_g$  of the CA/NYL66 (95/5) blend membrane is 249.86°C, which is higher compared to that of the neat CA membrane (246.28°C). The  $T_g$  of the CA pure membrane is largely in line with the previously reported results from other research works [37]. The addition of NYL66 up to 5 wt.% resulted in slight increase in the  $T_g$ , which is likely due to the increase in the crystallinity of the material. In other words, the chemical network formation of two polymers increases the  $T_g$  of blend polymers.

### 3.4. TGA studies

The weight loss of polymer materials in terms of temperature can be measured using TGA which is considered as an appropriate method for quantitative analysis of desorption, decomposition, and degradation procedures [49]. Fig. 6 displays the TGA curves for the pure membranes and the CA/NYL66 (95/5) blend membrane. All three demonstrated TGA curves present two degradation steps, after the evaporation of the solvent and water molecules at about 70°C. In the TGA curve of the pure NYL66 membrane, the highest rate of weight loss, about 85%, occurred in the first stage of degradation in the range of about 390°C–490°C, which could be attributed to the decomposition of the polymer. The second step of the decomposition between 500°C–720°C is related to the carbonization of degraded materials with a weight reduction of 10%, which shows the residual ash of the NYL66 is about 0.96%.

In the TGA graph of pure CA membrane, the first stage of decomposition causing the weight reduction of 77% is considered as the main part of polymer decomposition. It is between 270°C and 390°C followed by the second stage of decomposition at 400°C–580°C, which is in line with the existing literature in this regard [33].

The TGA curve of the CA/NYL66 (95/5) blend membrane has a similar trend to the CA membrane, with the

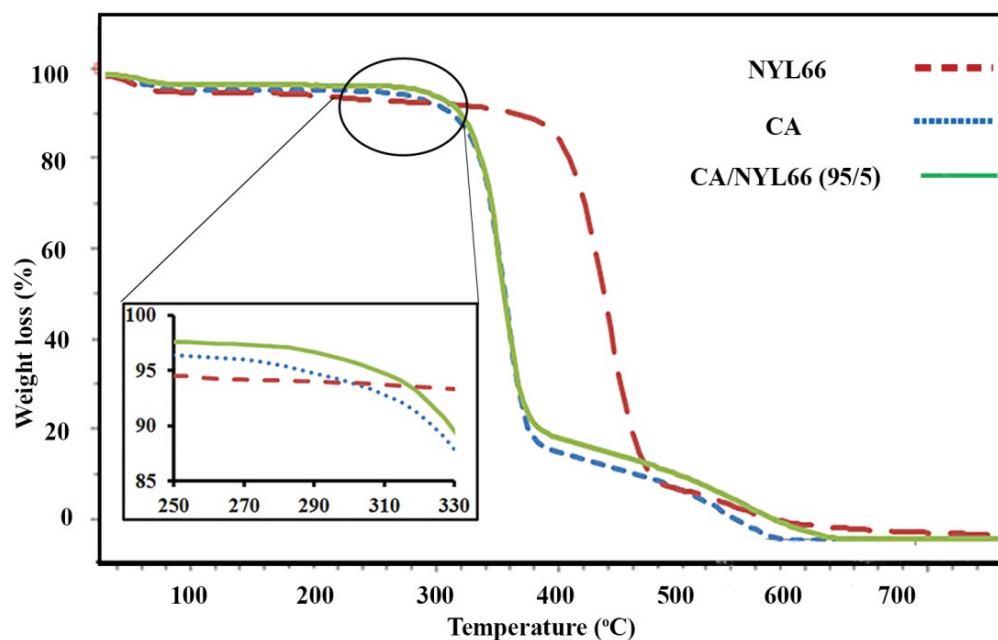


Fig. 6. TGA curves of the pure membranes and the CA/NYL66 (95/5) blend membrane.

only difference that in the former, the second decomposition stage finishes at 625°C. This amount of similarity can be attributed to the notable presence of CA in the CA/NYL66 (95/5) blend membrane. Additionally, polymer decomposition with a weight reduction of about 10% occurs at 332°C for the blended membrane and 327°C for the pure CA membrane which indicates an increase in the thermal stability of the blend membrane compared to that of the pure CA membrane. Higher thermal stability of the blend membrane is the result of a stronger interaction between the two polymers via forming of hydrogen bonding [25].

Fig. 7 shows the DTG graphs of the pure membranes and the CA/NYL66 (95/5) blend membrane. The maximum decomposition rate of the CA and CA/NYL66 (95/5) blend membranes occurs about 360°C, while that of the NYL66 membrane happens around 450°C. These results are in good agreement with the literature [50,51].

### 3.5. Contact angle of prepared membranes

Water contact angle measurement was conducted to investigate the hydrophilicity and surface wettability of the membranes. The results are illustrated in Fig. 8. The contact angle of the pure CA and NYL66 membrane was about 52.43°, similar to the result which exists in the literature [52], and 64.27°, respectively. As expected, the hydrophilic CA membrane had smaller water contact angle than that of the NYL66 membrane with lower hydrophilicity. According to the SEM images, the NYL66 membrane had a porous surface; therefore, its contact angle may be related to both hydrophilicity and top layer porosity. On the other hand, the SEM images of the pure CA membrane and the blend membranes showed completely dense surfaces, and the water contact angle in these membranes can only be attributed to their hydrophilicity.

The water contact angle of the blend membranes increased compared with that of the pure CA membrane, and therefore their hydrophilicity was reduced. It is noteworthy that the contact angle of the CA/NYL66 blend membranes was approximately enhanced by increasing the value of the NYL66, and the lowest contact angle (the highest

degree of hydrophilicity) was associated with the CA/NYL66 (95/5) blend membrane.

### 3.6. XRD analysis

The XRD spectra of the pure membranes and the CA/NYL66 (95/5) blend membrane are shown in Fig. 9. The pure NYL66 membrane exhibited a low-intensity peak at  $2\theta = 8.30^\circ$ , while the pure CA membrane and the CA/NYL66 (95/5) blend membrane displayed a dispersive peak at  $2\theta = 8^\circ$ . These peaks could be attributed to the functional groups of N–H in NYL66 and O–H in CA [39].

The pure NYL66 also had an almost broad peak at  $2\theta = 13.50^\circ$  and two distinct diffraction peaks at  $2\theta = 20.18^\circ$  and  $24.34^\circ$  which can in turn specify the reflection of oriented ( $h\ l\ k$ ) planes and also a polymeric phase. For example, diffraction angle at  $13.50^\circ$ ,  $20.18^\circ$ , and  $24.34^\circ$  can be assigned to (0 0 2) plane and  $\gamma_1$ -phase, (1 0 0) plane and  $\alpha_1$ -phase, and finally (0 1 0) and (1 1 0) planes and  $\alpha_2$ -phase, respectively [37]. The  $\alpha$ -phase in NYL66 has unit cells with triclinic crystalline structure, which  $\alpha_1$ -phase is representative of the distance between the chains of bonded-hydrogen sheets and  $\alpha_2$ -phase is associated with the distance between sheets [37,47].

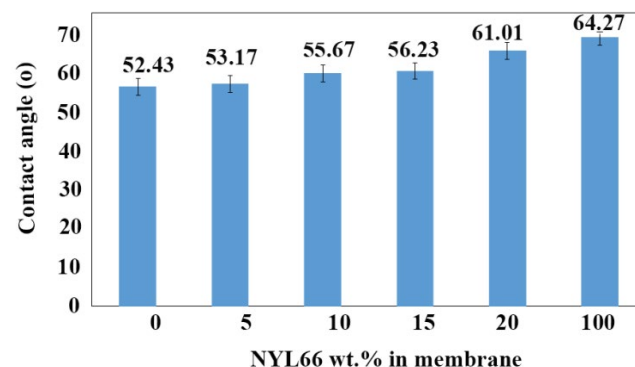


Fig. 8. Contact angle of prepared membranes in term of NYL66 wt.% in membrane.

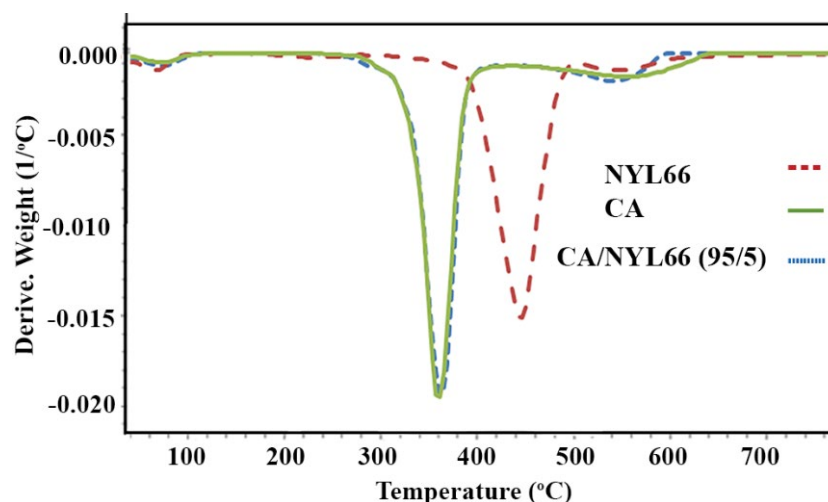


Fig. 7. DTG curves of the pure membranes and the CA/NYL66 (95/5) blend membrane.

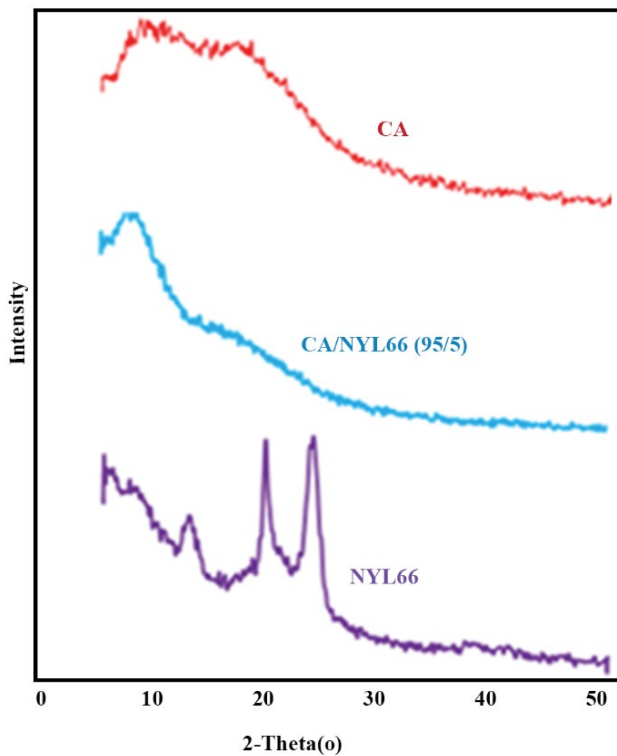


Fig. 9. X-ray diffraction patterns of the pure membranes and the CA/NYL66 (95/5) blend membrane.

### 3.7. Swelling measurements

The degree of swelling (%) was plotted as a function of NYL66 wt.% in the membranes (Fig. 10). As can be observed, the swelling degree of the CA/NYL66 blend membranes declined compared to that of the pure CA membrane, which could be related to the occurrence of the hydrogen bonding between the hydroxyl and amide functional groups.

In fact, NYL66 prevents further swelling due to its semi-crystalline nature and is not easily soluble in organic solvents. In other words, crystals perform the role of a crosslinker and reduce feed dissolution into the membrane, which occurs in the amorphous region [53]. However, the extent of swelling raised with increasing the NYL66 content up to 20 wt.% in the blend membrane. Since the IPA molecules and the NYL66 polymeric chain have both a polar (O–H in IPA and N–H in NYL66) and nonpolar (the carbon section in IPA and the main chain of the NYL66 polymer) segments, with an increase in the NYL66 ratio, the affinity of IPA and NYL66 molecules increases in the blend membranes and their interactions can lead to minor swelling.

### 3.8. Performance of prepared membranes in pervaporation process

Pervaporation experiments were performed using the prepared membranes for dehydration of IPA aqueous solution. Table 1 and Fig. 11 show the performance results as a function of the NYL66 content in the membranes. The concentrations and fluxes, listed in Table 1, indicate that all membranes are water selective, which according to the results of the contact angle, can be due to their hydrophilicity.

On the other hand, based on the results in this table, the increase of the NYL66 in the blend membrane led to a decrease in the concentration of water molecules in the permeate, whereas among all membranes, the highest water concentration in the permeate was related to the CA/NYL66 (95/5) blend membrane.

With respect to Table 1 and Fig. 11, in the pure CA membrane, the normalized flux and separation factor were  $4,209 \text{ g } \mu\text{m}^{-2} \text{ h}^{-1}$  and 387, respectively. As described in swelling section, the CA membrane had the largest swelling degree which can provide further paths for pass of the molecules through the membrane and then causes the increase of the total flux and the reduction of the separation factor. As observed, all blend membranes exhibited lower total flux than the pure CA membrane, which can be associated with the decrease in the swelling degree of blend membranes due to the existence of NYL66, as a semi-crystalline polymer, and a lack of flexible groups in crystals [53]. According to the DSC and XRD studies, the structure of NYL66 is semi-crystalline. Thus increasing the presence of NYL66 in the blend membrane increases the crystalline nature of the membranes.

The increase of NYL66 content, from 5 to 20 wt.%, in the blend membranes enhanced the affinity between IPA molecules in the feed (containing 80 wt.% IPA) and the blend membrane which led to an increase in the swelling, total flux, and partial flux. Among the blend membranes, CA/NYL66 (95/5) had the lowest affinity and consequently, the lowest swelling and flux. On the other hand, since CA/NYL66 (95/5) showed the lowest contact angle (the highest degree of hydrophilicity) among all blend membranes, a significant percentage of permeate flow (99.80 wt.%) belonged to the water molecules, and the value of separation factor was noticeably enhanced and reached 1,952 (Table 1 and Fig. 11). In other words, with the addition of NYL66 to 5 wt.%, the low affinity between IPA molecules and the blend membrane decreased the swelling and the flux, and the high hydrophilicity of CA/NYL66 blend membrane improved the separation factor. After more increasing the NYL66 percentage, from 5 to 20 wt.%, water concentration was decreased meanwhile IPA concentration was increased in permeate flow so that the separation factor was declined. It was confirmed that swollen membrane accelerates the diffusion of feed components within the membrane which leads to the increment of permeation flux and the decrement

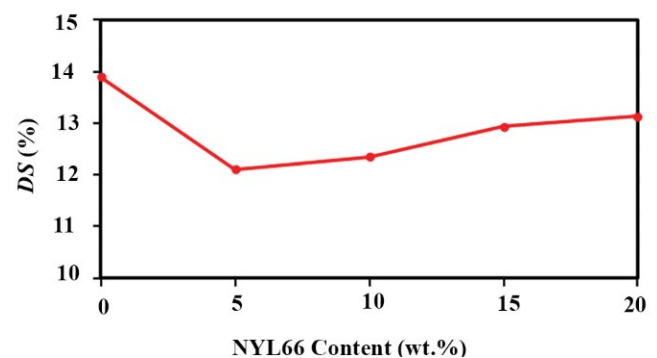


Fig. 10. Swelling degree of the prepared membranes.

Table 1  
Values of fluxes and permeate concentration

NYL66 wt.% in membrane	0	5	10	15	20
Water concentration in permeate (wt.%)	98.98	99.80	99.39	99.18	96.33
IPA concentration in permeate (wt.%)	1.02	0.20	0.61	0.82	3.67
Normalized water flux ( $\text{g } \mu\text{m}^{-2} \text{h}^{-1}$ )	4,165.98	2,653.52	2,934.97	3,171.81	3,507.33
Normalized IPA flux ( $\text{g } \mu\text{m}^{-2} \text{h}^{-1}$ )	43.02	5.44	18.11	26.15	133.62
Normalized total flux ( $\text{g } \mu\text{m}^{-2} \text{h}^{-1}$ )	4,209.00	2,658.96	2,953.08	3,197.96	3,640.95

Table 2  
Pervaporation performance of CA-based membranes in dehydration of IPA

Membrane	Pervaporation temperature ( $^{\circ}\text{C}$ )	Feed composition (wt.% water)	Total flux ( $\text{g m}^{-2} \text{h}$ )	Separation factor	Reference
CA	40	75	~200	~650	[33]
CA/PEG	40	75	~230	~640	[33]
CA/EG	40	75	~350	~410	[33]
CA/PG	40	75	~280	~600	[33]
CA/ZnO	40	71	~559	~1,448	[34]
CA/NYL66 (95/5)	30	80	~108	~1,952	Present work

of separation factor of the membrane. In fact, the increase in swelling degree causes the plasticity of the surface layer of the membrane and has a negative effect on the membrane selectivity so that membrane layer would allow passing further IPA molecules along with water molecules [18].

The overall performance of the prepared membranes in pervaporation is estimated by PSI, which includes both the total flux and separation factor. Fig. 11 shows the PSI values for the prepared membranes as an overall index which exhibit the total performance of pervaporation separation. Based on the gained results here, the CA/NYL66 (95/5) had the best separation performance. In completion of the present work, the effect of different conditions on pervaporation dehydration in CA/NYL66 (95/5) membrane, as an optimal blend membrane, was investigated in our recent work [54].

### 3.9. Comparison with other studies

The pervaporation performance of the CA/NYL66 blend membrane was compared with other CA-based blend membranes in dehydration of IPA in Table 2. As indicated in the table, the CA/NYL66 blend membrane with 95 wt.% CA in the present work had a high separation factor of water/IPA and provided a reasonable flux at  $30^{\circ}\text{C}$  which can decrease the energy consumption during heating of the feed compared to other results.

## 4. Conclusions

The pure CA and NYL66 membranes and also the CA/NYL66 blend membranes with different ratios of the CA/NYL66 were successfully prepared and used for IPA dehydration. SEM images from the surface of the membranes showed that the pure NYL66 membrane was completely

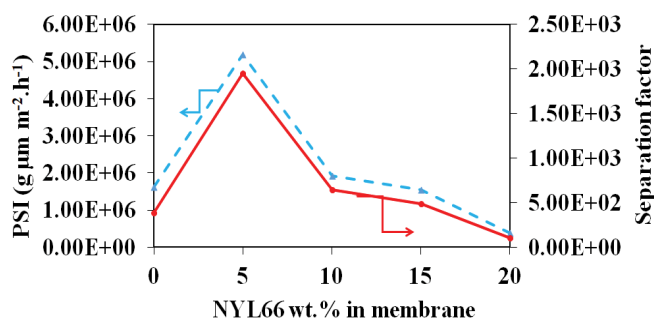


Fig. 11. Values of PSI and separation factor for the prepared membranes.

porous, whereas the blend membranes and the pure CA membrane had a very compact and dense surface and were appropriate for the pervaporation process. In addition, the cross-sectional area of the blend membranes had a denser structure than the pure NYL66 membrane.

The FTIR results of the membranes implied the formation of an intermolecular force of hydrogen bonding between CA and NYL66 polymers, which indicates the appropriate miscibility between the two polymers. Moreover, the thermal stability of the blend CA/NYL66 (95/5) membrane improved compared with that of the pure CA membrane.

Finally, pervaporation and swelling experiments illustrated that the blend CA/NYL66 (95/5) membrane containing the least degree of swelling showed the best pervaporation separation performance in dehydration of IPA with the separation factor of about 1,952 and total normalized flux of  $2,659 \text{ g } \mu\text{m}^{-2} \text{h}^{-1}$ . These results were highly accordance with other results such as contact angles measurements.

## Symbols

$A$	— Effective membrane area, $m^2$
$\Delta H_f$	— Enthalpy of melting, $J g^{-1}$
$\Delta H_{f100\%}$	— Enthalpy of melting for a fully crystalline NYL66, $J g^{-1}$
DS (%)	— Degree of swelling, —
$J$	— Normalized flux, $g \mu m^{-2} h^{-1}$
$l$	— Membrane thickness, $\mu m$
$m$	— Mass of permeate, $g$
PSI	— Performance of pervaporation separation, $g \mu m^{-2} h^{-1}$
$t$	— Time, $h$
$W_d$	— Weight of the membrane in the dry stat, $g$
$W_s$	— Weight of the membrane in the swollen state, $g$
$X_i$	— Weight fraction of isopropanol in the feed, —
$X_w$	— Weight fraction of water in the feed, —
$Y_i$	— Weight fraction of isopropanol in the permeate, —
$Y_w$	— Weight fraction of water in the permeate, —

## Greek symbols

$\alpha$	— Separation factor, —
----------	------------------------

## Subscripts

$d$	— Dried membrane
$i$	— Isopropanol
$s$	— Swollen membrane
$w$	— Water

## Abbreviations

CA	— Cellulose acetate
FA	— Formic acid
FTIR	— Fourier transform infrared spectroscopy
IPA	— Isopropanol
NYL66	— Nylon 66
SEM	— Scanning electron microscopy
TGA/DSC	— Thermogravimetric analysis and differential scanning calorimetry
XRD	— X-ray diffraction

## References

- [1] Y.M. Xu, T.S. Chung, High-performance UiO-66/polyimide mixed matrix membranes for ethanol, isopropanol and n-butanol dehydration via pervaporation, *J. Membr. Sci.*, 531 (2017) 16–26.
- [2] A.C. Duque Salazar, M.A. Gómez García, J. Fontalvo, M. Jedrzejczyk, J.M. Rynkowski, I. Dobrosz-Gómez, Ethanol dehydration by pervaporation using microporous silica membranes, *Desal. Water Treat.*, 51 (2013) 2368–2376.
- [3] Z. Mao, Y. Cao, X. Jie, G. Kang, M. Zhou, Q. Yuan, Dehydration of isopropanol–water mixtures using a novel cellulose membrane prepared from cellulose/N-methylmorpholine-N-oxide/ $H_2O$  solution, *Sep. Purif. Technol.*, 72 (2010) 28–33.
- [4] F. Ugur Nigiz, N. Durmaz Hilmioglu, Pervaporation of ethanol/water mixtures by zeolite filled sodium alginate membrane, *Desal. Water Treat.*, 51 (2013) 637–643.
- [5] Y. Zhu, S. Xia, G. Liu, W. Jin, Preparation of ceramic-supported poly (vinyl alcohol) – chitosan composite membranes and their applications in pervaporation dehydration of organic /water mixtures, *J. Membr. Sci.*, 349 (2010) 341–348.
- [6] A. Malekpour, B. Mostajeran, G.A. Koohmareh, Pervaporation dehydration of binary and ternary mixtures of acetone, isopropanol and water using polyvinyl alcohol/zeolite membranes, *Chem. Eng. Process.*, 118 (2017) 47–53.
- [7] L. Gao, M. Alberto, P. Gorgojo, G. Szekely, P.M. Budd, High-flux PIM-1/PVDF thin film composite membranes for 1-butanol/water pervaporation, *J. Membr. Sci.*, 529 (2017) 207–214.
- [8] H. Yin, C.Y. Lau, M. Rozowski, C. Howard, Y. Xu, T. Lai, M.E. Dose, R.P. Lively, M.L. Lind, Free-standing ZIF-71/PDMS nanocomposite membranes for the recovery of ethanol and 1-butanol from water through pervaporation, *J. Membr. Sci.*, 529 (2017) 286–292.
- [9] S. Soloukipour, E. Saljoughi, S.M. Mousavi, PEBA/PVDF blend pervaporation membranes: preparation and performance, *Polym. Adv. Technol.*, 28 (2017) 113–123.
- [10] Y. Zhang, N. Wang, C. Zhao, L. Wang, S. Ji, J.R. Li, Co(HCOO)<sub>2</sub>-based hybrid membranes for the pervaporation separation of aromatic/aliphatic hydrocarbon mixtures, *J. Membr. Sci.*, 520 (2016) 646–656.
- [11] H. Abdallah, A. El-Gendi, E. El-Zanati, T. Matsuura, Pervaporation of methanol from methylacetate mixture using polyamide-6 membrane, *Desal. Water Treat.*, 51 (2013) 7807–7814.
- [12] B. Smitha, D. Suhanya, S. Sridhar, M. Ramakrishna, Separation of organic–organic mixtures by pervaporation – a review, *J. Membr. Sci.*, 241 (2004) 1–21.
- [13] H. Sardarabadi, S.M. Mousavi, E. Saljoughi, Removal of 2-propanol from water by pervaporation using poly (vinylidene fluoride) membrane filled with carbon black, *Appl. Surf. Sci.*, 368 (2016) 277–287.
- [14] S. Araki, S. Imasaka, S. Tanaka, Y. Miyake, Pervaporation of organic/water mixtures with hydrophobic silica membranes functionalized by phenyl groups, *J. Membr. Sci.*, 380 (2011) 41–47.
- [15] B.V.D. Bruggen, P. Luis, E.S. Tarleton, ed., *Filtration and Separation Progress*, Academic Press, London 2015, pp. 101–144.
- [16] Q.G. Zhang, Q.L. Liu, Y. Chen, J.H. Chen, Dehydration of isopropanol by novel poly (vinyl alcohol)-silicone hybrid membranes, *Ind. Eng. Chem. Res.*, 46 (2007) 913–920.
- [17] Q. Zhao, J. Qian, Q. An, Z. Gui, H. Jin, M. Yin, Pervaporation dehydration of isopropanol using homogeneous polyelectrolyte complex membranes of poly(diallyldimethylammonium chloride)/sodium carboxymethyl cellulose, *J. Membr. Sci.*, 329 (2009) 175–182.
- [18] S. Langari, E. Saljoughi, S.M. Mousavi, Chitosan/polyvinyl alcohol/amino functionalized multiwalled carbon nanotube pervaporation membranes: synthesis, characterization, and performance, *Polym. Adv. Technol.*, 29 (2018) 84–94.
- [19] S.B. Teli, G.S. Gokavi, T.M. Tak, T.M. Aminabhavi, Chitosan/gelatin blend membranes for pervaporation dehydration of 1,4-Dioxane, *Sep. Sci. Technol.*, 44 (2009) 3202–3223.
- [20] P. Das, S.K. Ray, Synthesis of highly water selective copolymer membranes for pervaporative dehydration of acetonitril, *J. Membr. Sci.*, 507 (2016) 81–89.
- [21] C. Yu, C. Zhong, Y. Liu, X. Gu, G. Yang, W. Xing, N. Xu, Pervaporation dehydration of ethylene glycol by NaA zeolite membranes, *Chem. Eng. Res. Des.*, 90 (2012) 1372–1380.
- [22] H.A. Magosso, N. Fattori, L.T. Arenas, Y. Gushikem, New promising composite materials useful in the adsorption of Cu(II) in ethanol based on cellulose and cellulose acetate, *Cellulose*, 19 (2012) 913–923.
- [23] Y. Miyashita, T. Suzuki, Y. Nishio, Miscibility of cellulose acetate with vinyl polymers, *Cellulose*, 9 (2002) 215–223.
- [24] K. Zhou, Q.G. Zhang, G.L. Han, A.M. Zhu, Q. L. Liu, Pervaporation of water–ethanol and methanol–MTBE mixtures using poly (vinyl alcohol)/cellulose acetate blended membranes, *J. Membr. Sci.*, 448 (2013) 93–101.
- [25] H. Wu, X. Fang, X. Zhang, S. Jiang, B. Li, X. Ma, Cellulose acetate-poly (N-vinyl-2-pyrrolidone) blend membrane for pervaporation separation of methanol/MTBE mixtures, *Sep. Purif. Technol.*, 64 (2008) 183–191.

- [26] G.M. Shashidhara, K.H. Guruprasad, A. Varadarajulu, Miscibility studies on blends of cellulose acetate and nylon 6, *Eur. Polym. J.*, 38 (2002) 611–614.
- [27] M.G.M. Nawawi, Pervaporation Dehydration of Isopropanol-Water Systems Using Chitosan Membranes, Ph.D. Thesis, University of Waterloo, 1997.
- [28] W.F. Guo, Pervaporation study of butanol/water mixtures by polyvinylalcohol (PVA) and polyimide membranes, Ph.D. Thesis, National University of Singapore, 2007.
- [29] S. Vetrivel, D. Rana, M.S.A. Saraswathi, K. Divya, N.J. Kaleekkal, A. Nagendran, Cellulose acetate nanocomposite ultrafiltration membranes tailored with hydrous manganese dioxide nanoparticles for water treatment applications, *Polym. Adv. Technol.*, 30 (2019) 1943–1950.
- [30] M.S.A. Saraswathi, A. Nagendran, D. Rana, Tailored polymer nanocomposite membranes based on carbon, metal oxide and silicon nanomaterials: a review, *J. Mater. Chem. A*, 7 (2019) 8723–8745.
- [31] M. Niang, G. Luo, P. Schaetzel, Pervaporation separation of methyl tert-butyl ether/methanol mixtures using a high-performance blended, *J. Appl. Polym. Sci.*, 64 (1997) 875–882.
- [32] J.H. Lv, G.M. Xiao, Dehydration of water/pyridine mixtures by pervaporation using cellulose acetate/polyacrylonitrile blend membrane, *Water Sci. Technol.*, 63 (2011) 1695–1700.
- [33] M. Zafar, M. Ali, S.M. Khan, T. Jamil, M.T.Z. Butt, Effect of additives on the properties and performance of cellulose acetate derivative membranes in the separation of isopropanol/water mixtures, *Desalination*, 285 (2012) 359–365.
- [34] M. Ali, M. Zafar, T. Jamil, M.T.Z. Butt, Influence of glycol additives on the structure and performance of cellulose acetate/zinc oxide blend membranes, *Desalination*, 270 (2011) 98–104.
- [35] S. Deng, B. Shiyao, S. Sourirajan, T. Matsuura, A study of the pervaporation of isopropyl alcohol/water mixtures by cellulose acetate membranes, *J. Colloid Interface Sci.*, 136 (1990) 283–291.
- [36] H.A. Tsai, H.C. Chen, W.L. Chou, K.R. Lee, M.C. Yang, J.Y. Lai, Pervaporation of water/alcohol mixtures through chitosan/cellulose acetate composite hollow-fiber membranes, *J. Appl. Polym. Sci.*, 94 (2004) 1562–1568.
- [37] A. Linggawati, A.W. Mohammad, C.P. Leo, Effects of APTEOS content and electron beam irradiation on physical and separation properties of hybrid nylon-66 membranes, *Mater. Chem. Phys.*, 133 (2012) 110–117.
- [38] X.P. Zhao, R.Y.M. Huang, Pervaporation separation of ethanol-water mixtures using crosslinked blended polyacrylic acid (PAA)-nylon 66 membranes, *J. Appl. Polym. Sci.*, 41 (1990) 2133–2145.
- [39] S. Sridhar, B. Smitha, A.A. Reddy, Separation of 2-butanol-water mixtures by pervaporation through PVA-NYL 66 blend membranes, *Colloids Surf., A*, 280 (2006) 95–102.
- [40] B. Smitha, G. Dhanuja, S. Sridhar, Dehydration of 1,4-dioxane by pervaporation using modified blend membranes of chitosan and nylon 66, *Carbohydr. Polym.*, 66 (2006) 463–472.
- [41] X. Yan, H. Ye, C. Dong, Y. Wu, S. Shi, preparation and characterization of PIM-1/PU-blend membranes for pervaporation separation of phenol from water, *Desal. Water Treat.*, 138 (2019) 68–79.
- [42] M. Balakrishnan, R.Y.M. Huang, Pervaporation separation of pentane-alcohol mixtures through ionically crosslinked blended membranes, *Angew. Makromol. Chem.*, 191 (1991) 39–69.
- [43] H. Kamal, F.M. Abd-Elrahim, S. Lotfy, Characterization and some properties of cellulose acetate-co-polyethylene oxide blends prepared by the use of gamma irradiation, *J. Radiat. Res. Appl. Sci.*, 7 (2014) 146–153.
- [44] J.A. Sánchez-Márquez, R. Fuentes-Ramírez, I. Cano-Rodríguez, Z. Gamiño-Arroyo, E. Rubio-Rosas, J. M. Kenny and N. Rescignano, Membrane made of cellulose acetate with polyacrylic acid reinforced with carbon nanotubes and its applicability for chromium removal, *Int. J. Polym. Sci.*, 2015 (2015) 1–12.
- [45] M. Montazer, M. Parvinzadeh, Effect of ammonia on madder-dyed natural protein fiber, *J. Appl. Polym. Sci.*, 93 (2004) 2704–2710.
- [46] J. Charles, G.R. Ramkumaar, S. Azhagiri, S. Gunasekaran, FTIR and thermal studies on nylon-66 and 30% glass fibre reinforced nylon-66, *J. Chem.*, 6 (2009) 23–33.
- [47] F. Navarro-Pardo, G. Martínez-barrera, A.L. Martínez-Hernández, V.M. Castaño, J.L. Rivera-Armenta, F. Medellín-Rodríguez, C. Velasco-Santos, Effects on the thermomechanical and crystallinity properties of nylon 6,6 electrospun fibres reinforced with one dimensional (1D) and two dimensional (2D) carbon, *Materials*, 6 (2013) 3494–3513.
- [48] D.J. Lin, C.L. Chang, C.K. Lee, L.P. Cheng, Fine structure and crystallinity of porous nylon 66 membranes prepared by phase inversion in the water/formic acid/nylon 66 system, *Eur. Polym. J.*, 42 (2006) 356–367.
- [49] Z.S. Kalkan, The Generation and Thermo-Mechanical Characterization of Advanced Polyamide 6,6 Nanocomposites Using Interfacial Polycondensation, Ph.D. Thesis, University of Akron, 2006.
- [50] C.H. Worthley, K.T. Constantopoulos, M. Ginic-Markovic, E. Markovic, S. Clarke, A study into the effect of POSS nanoparticles on cellulose acetate membranes, *J. Membr. Sci.*, 431 (2013) 62–71.
- [51] D. Zavastin, I. Cretescu, M. Bezdadea, M. Bourceanu, M. Dragan, G. Lisa, I. Mangalagiu, V. Vasic, J. Savic, Preparation, characterization and applicability of cellulose acetate-polyurethane blend membrane in separation techniques, *Colloids Surf., A*, 370 (2010) 120–128.
- [52] I. Guezguez, B. Mrabet, E. Ferjani, XPS and contact angle characterization of surface modified cellulose acetate membranes by mixtures of PMHS/PDMS, *Desalination*, 313 (2013) 208–211.
- [53] M.K. Buckley-Smith, The Use of Solubility Parameters to Select Membrane Materials for Pervaporation of Organic Mixtures, Ph.D. Thesis, University of Waikato, Hamilton, New Zealand, 2006.
- [54] A. Kazemzadeh, S.M. Mousavi, J. Mehrzad, A. Motavallizadehkakhky, M. Hosseiny, Effect of different conditions on pervaporation dehydration in CA/NYL66 blend membrane, *Membr. Water Treat.*, 10 (2019) 441–449.